

## Enhanced Hydrogen Storage Capacity of High Surface Area Zeolite-like Carbon Materials

Zhuxian Yang, Yongde Xia, and Robert Mokaya\*

Contribution from the School of Chemistry, University of Nottingham,  
Nottingham NG7 2RD, United Kingdom

Received October 5, 2006; E-mail: r.mokaya@nottingham.ac.uk

**Abstract:** We report the synthesis of zeolite-like carbon materials that exhibit well-resolved powder XRD patterns and very high surface area. The zeolite-like carbons are prepared via chemical vapor deposition (CVD) at 800 or 850 °C using zeolite  $\beta$  as solid template and acetonitrile as carbon precursor. The zeolite-like structural ordering of the carbon materials is indicated by powder XRD patterns with at least two well-resolved diffraction peaks and TEM images that reveal well-ordered micropore channels. The carbons possess surface area of up to 3200 m<sup>2</sup>/g and pore volume of up to 2.41 cm<sup>3</sup>/g. A significant proportion of the porosity in the carbons (up to 76% and 56% for surface area and pore volume, respectively) is from micropores. Both TEM and nitrogen sorption data indicate that porosity is dominated by pores of size 0.6–0.8 nm. The carbon materials exhibit enhanced (and reversible) hydrogen storage capacity, with measured uptake of up to 6.9 wt % and estimated maximum of 8.33 wt % at –196 °C and 20 bar. At 1 bar, hydrogen uptake capacity as high as 2.6 wt % is achieved. Isotheric heat of adsorption of 8.2 kJ/mol indicates a favorable interaction between hydrogen and the surface of the carbons. The hydrogen uptake capacity observed for the zeolite-like carbon materials is among the highest ever reported for carbon (activated carbon, mesoporous carbon, CNTs) or any other (MOFs, zeolites) porous material.

### 1. Introduction

Porous inorganic solids such as zeolites and mesoporous silicas have been extensively used as hard templates for the preparation of nanoporous carbon materials. The porous carbons are obtained via the template carbonization method, which involves the introduction of suitable carbon precursors into the pores of a hard template followed by carbonization and finally removal of the template.<sup>1,2</sup> In general, the use of zeolites and mesoporous silicas as hard templates results in microporous or mesoporous carbons, respectively.<sup>1,2</sup> However, while the structural ordering of mesoporous carbons is usually a faithful replica of the pore channel ordering of the silica templates, it is much more difficult to replicate the zeolite pore structure. The XRD patterns of mesoporous carbons therefore exhibit several diffraction peaks arising from mesostructural ordering, while the XRD patterns of zeolite-templated carbons occasionally have

only one weak diffraction peak.<sup>1,2</sup> The poor replication of the zeolite structure in carbons has been attributed to several reasons including low carbon loading due to the small pore size of zeolites, or disorder/inappropriate symmetry of the zeolite pore ordering.<sup>3,4</sup> In particular, the close replication of the pore ordering of zeolite  $\beta$  and zeolite Y in carbons is considered to be difficult due to the disordered structure of zeolite  $\beta$  and high-symmetry cubic space group in zeolite Y.<sup>3,4</sup> To circumvent this difficulty, Parmentier and co-workers considered it essential to use a large pore zeolite with a two- or three-dimensional non-cubic pore system (e.g., zeolite EMC-2) as template and succeeded in preparing a zeolite carbon replica with more than one XRD peak.<sup>4</sup> This, however, has the unattractive implication that only a limited number of zeolites may be used to give faithful replica carbons.

It is therefore desirable to explore nanocasting routes, which may more generally generate carbons with well-resolved XRD patterns from commercially available zeolite templates with disordered structures such as zeolite  $\beta$ . Disordered zeolite structures are those that show periodic ordering in less than three dimensions (i.e., 2, 1, or 0 dimensions). In this regard, zeolite  $\beta$  is considered to have a disordered structure because it typically consists of an intergrowth of at least two distinct structures, polymorphs A and B. The polymorphs, which both possess a three-dimensional network of pores, grow as randomly alternating two-dimensional sheets. The intergrowth causes stacking

\* Corresponding author.

- (1) (a) Ryoo, R.; Joo, S. H.; Kruk, M.; Jaroniec, M. *Adv. Mater.* **2001**, *13*, 677. (b) Ryoo, R.; Joo, S. H.; Jun, S. J. *Phys. Chem. B* **1999**, *103*, 7743. (c) Jun, S.; Joo, S. H.; Ryoo, R.; Kruk, M.; Jaroniec, M.; Liu, Z.; Ohsuna, T.; Terasaki, O. *J. Am. Chem. Soc.* **2000**, *122*, 10712. (d) Lee, J.; Han, S.; Hyeon, T. *J. Mater. Chem.* **2004**, *14*, 478. (e) Yang, H. F.; Zhao, D. Y. *J. Mater. Chem.* **2005**, *15*, 1217. (f) Lee, J.; Kim, J.; Hyeon, T. *Adv. Mater.* **2006**, *18*, 2073.
- (2) (a) Johnson, S. A.; Brigham, E. S.; Ollivier, P. J.; Mallouk, T. E. *Chem. Mater.* **1997**, *9*, 2448. (b) Kyotani, T.; Nagai, T.; Inoue, S.; Tomita, A. *Chem. Mater.* **1997**, *9*, 609. (c) Rodriguez-Mirasol, J.; Cordero, T.; Radovic, L. R.; Rodriguez, J. J. *Chem. Mater.* **1998**, *10*, 550. (d) Barata-Rodrigues, P. M.; Mays, T. J.; Moggridge, G. D. *Carbon* **2003**, *41*, 2231. (e) Meyers, C. J.; Shah, S. D.; Patel, S. C.; Sneeinger, R. M.; Bessel, C. A.; Dollahon, N. R.; Leising, R. A.; Takeuchi, E. S. *J. Phys. Chem. B* **2001**, *105*, 2143. (f) Su, F.; Zhao, X. S.; Lu, L.; Zhou, Z. *Carbon* **2004**, *42*, 2821. (g) Bandosz, T. J.; Jagiello, J.; Putyera, K.; Schwarz, J. A. *Chem. Mater.* **1996**, *8*, 2023.

(3) Kyotani, T.; Ma, Z. X.; Tomita, A. *Carbon* **2003**, *41*, 1451.

(4) Gaslain, F. O. M.; Parmentier, J.; Valtchev, V. P.; Patarin, J. *Chem. Commun.* **2006**, 991.

faults with the overall effect being that the pores of zeolite  $\beta$ , rather than being fully three-dimensionally ordered, are two-dimensionally ordered with some stacking disorder in the third direction.

Porous carbons with well-ordered pore systems are potentially useful as gas storage materials.<sup>5</sup> Of particular interest is hydrogen storage, which is relevant to the anticipated hydrogen economy where hydrogen may be used as a source of energy. The hydrogen sorption capacity of porous carbons generally increases with surface area.<sup>6</sup> It is therefore desirable to prepare high surface area carbon materials. The preparation of structurally zeolite-like carbons with well-resolved XRD peaks may offer a route to high surface area materials with high hydrogen sorption capacity. Here, we demonstrate the first synthesis of structurally zeolite-like carbon materials with well-resolved XRD patterns using zeolite  $\beta$  as template. The zeolite-like (with respect to structural pore ordering) carbons are obtained by using zeolite  $\beta$  as template and chemical vapor deposition (CVD) to deposit the carbon precursor into the pores of the zeolite. Our findings show that zeolite  $\beta$  can be used as template to nanocast ordered zeolite-like carbons with well-resolved XRD patterns arising from a high level of zeolite-type structural ordering and that the carbon materials possess very high surface area and enhanced hydrogen uptake capacity.

## 2. Experimental Section

**2.1. Material Synthesis.** The zeolite  $\beta$  templates were obtained using established procedures.<sup>7</sup> Carbon materials were prepared via CVD by placing an alumina boat with 0.5 g of zeolite in a flow through tube furnace, which was then heated to 800 or 850 °C under nitrogen flow. Once the target temperature was attained, the flow of nitrogen was switched to nitrogen saturated with acetonitrile (the carbon precursor) for a heating period of 3 h at the target temperature. The resulting zeolite/carbon composites were recovered and washed with 10% hydrofluoric (HF) acid several times to remove the zeolite framework. Finally, the resulting carbon materials were dried in an oven at 120 °C. (Thermogravimetric analysis of the HF-treated carbons indicated a residual mass typically lower than 3% at 800 °C, which indicated that the carbon materials were virtually zeolite free.) We note that the use of acetonitrile as carbon source resulted in nitrogen-containing (N-doped) carbons. The amount and nature of the nitrogen in acetonitrile-derived carbons have been extensively investigated in previous reports.<sup>8–10</sup> Two zeolite  $\beta$  templates designated as ZTA and ZTB were used. ZTA was used to generate two samples, designated as CA800

and CA850, at CVD temperatures of 800 and 850 °C, respectively. ZTB generated sample CB850 at a CVD temperature of 850 °C. A further sample (designated as CB850h) was prepared from ZTB by subjecting the zeolite/carbon composite obtained after the CVD step to further heat treatment under nitrogen flow for 3 h (i.e., heat treatment in the absence of acetonitrile).

**2.2. Material Characterization.** Powder XRD analysis was performed using a Philips 1830 powder diffractometer with Cu K $\alpha$  radiation (40 kV, 40 mA), 0.02° step size, and 2 s step time. Textural properties were determined via nitrogen sorption at –196 °C using a conventional volumetric technique on an ASAP 2020 sorptometer. Before analysis, the samples were oven-dried at 130 °C and evacuated for 12 h at 200 °C under vacuum. The surface area was calculated using the Brunauer–Emmett–Teller (BET) method based on adsorption data in the partial pressure ( $P/P_0$ ) range 0.02–0.25, and total pore volume was determined from the amount of nitrogen adsorbed at  $P/P_0 = \text{ca. } 0.99$ . Although the BET method has limitations with respect to calculating the surface area of microporous materials, it is suitably used here for comparative analysis of the surface area of a set of comparable samples. The partial pressure range,  $P/P_0 = 0.02–0.25$ , for the calculation of surface area was selected taking into account previous reports that indicate that using low partial pressure range,  $P/P_0 = 0.01–0.05$ , overestimates the surface area while using the partial pressure range  $P/P_0 = 0.1–0.3$  can underestimate the surface area.<sup>4,11</sup> Scanning electron microscopy (SEM) images were recorded using a JEOL JSM-820 scanning electron microscope. Transmission electron microscopy (TEM) images were recorded on a JEOL 2000-FX electron microscope operating at 200 kV.

**2.3. Hydrogen Uptake Measurements.** Gravimetric determination of hydrogen uptake capacity was performed using an Intelligent Gravimetric Analyzer (IGA-003, Hiden), which incorporates a microbalance capable of measuring weights with a resolution of  $\pm 0.2 \mu\text{g}$ . Hydrogen uptake was determined at –196 °C over the pressure range 0–20 bar. The samples were outgassed ( $10^{-10}$  bar) under heating at 200 °C overnight before measurement. Hydrogen uptake capacity was also determined with a Micromeritics ASAP 2020 sorptometer (volumetric method) as follows. The samples were evacuated at 200 °C under vacuum overnight, and the hydrogen uptake was evaluated over the pressure range 0–1.1 bar at –196 °C. For both methods (gravimetric and volumetric), high-purity hydrogen (99.9999%) additionally purified by a molecular sieve filter was used for the uptake measurements.

## 3. Results and Discussion

**3.1. Zeolite-like Carbons.** The powder X-ray diffraction (XRD) patterns of zeolite  $\beta$  templates and corresponding carbon materials are shown in Figure 1. In Figure 1A, the XRD patterns of the carbon samples show a peak at  $2\theta = 7^\circ$  (hereinafter referred to as the basal peak). This “basal peak” is at the same position as the (100), (101) diffraction of the zeolite  $\beta$  template and therefore indicates that the carbon materials exhibit structural pore ordering similar to that of the zeolite with a “basal spacing” of ca. 1.2 nm.<sup>3,4,8</sup> The intensity of the “basal peak” suggests that zeolite-type structural ordering is better replicated in the carbons prepared at higher (850 vs 800 °C) CVD temperature. The XRD patterns exhibit a further peak at  $2\theta = 15^\circ$ , which is at a position similar to the (201), (202) diffraction of the zeolite  $\beta$  template. The second diffraction peak is consistent with a high level of replication of zeolite-type structural ordering in the carbons. The XRD patterns in Figure 1 are different from those previously observed for zeolite- $\beta$  templated carbon materials where only one weak “basal peak”

- (5) Dillon, A. C.; Jones, K. M.; Bekkedahl, T. A.; Kiang, C. H.; Bethune, D. S.; Heben, M. J. *Nature* **1997**, *386*, 377.
- (6) (a) Hirscher, M.; Panella, B. *J. Alloys Compd.* **2005**, *404*, 399. (b) Zhao, X. B.; Xiao, B.; Fletcher, A. J.; Thomas, K. M. *J. Phys. Chem. B* **2005**, *109*, 8880. (c) Pang, J.; Hampsey, J. E.; Wu, Z.; Hu, Q.; Lu, Y. *Appl. Phys. Lett.* **2004**, *85*, 4887. (d) Terres, E.; Panella, B.; Hayashi, T.; Kim, Y. A.; Endo, M.; Dominguez, J. M.; Hirscher, M.; Terrones, H.; Terrones, M. *Chem. Phys. Lett.* **2005**, *403*, 363. (e) Gogotsi, Y.; Dash, R. K.; Yushin, G.; Yildirim, T.; Laudisio, G.; Fischer, J. E. *J. Am. Chem. Soc.* **2005**, *127*, 16006. (f) Fang, B.; Zhou, H.; Honma, I. *J. Phys. Chem. B* **2006**, *110*, 4875. (g) Vix-Guterl, C.; Frackowiak, E.; Jurewicz, K.; Friebe, M.; Parmentier, J.; Beguin, F. *Carbon* **2005**, *43*, 1293. (h) Texier-Mandoki, N.; Dentzer, J.; Piquero, T.; Saadallah, S.; David, P.; Vix-Guterl, C. *Carbon* **2004**, *42*, 2744. (i) Zuttel, A.; Sudan, P.; Mauron, P.; Kiyobayashi, T.; Emmenegger, Ch.; Schlappbach, L. *Int. J. Hydrogen Energy* **2002**, *27*, 203.
- (7) Jones, C. W.; Tsuji, K.; Davis, M. E. *Microporous Mesoporous Mater.* **1999**, *33*, 223.
- (8) (a) Yang, Z.; Xia, Y.; Mokaya, R. *Microporous Mesoporous Mater.* **2005**, *86*, 69. (b) Yang, Z.; Xia, Y.; Mokaya, R. *Stud. Surf. Sci. Catal.* **2005**, *156*, 573.
- (9) Yang, Z.; Xia, Y.; Sun, X.; Mokaya, R. *J. Phys. Chem. B* **2006**, *110*, 18424.
- (10) (a) Xia, Y.; Mokaya, R. *Adv. Mater.* **2004**, *16*, 1553. (b) Xia, Y.; Yang, Z.; Mokaya, R. *J. Phys. Chem. B* **2004**, *108*, 19293. (c) Xia, Y.; Yang, Z.; Mokaya, R. *Stud. Surf. Sci. Catal.* **2005**, *156*, 565. (d) Xia, Y.; Mokaya, R. *Chem. Mater.* **2005**, *17*, 1553. (e) Xia, Y.; Yang, Z.; Mokaya, R. *Chem. Mater.* **2006**, *18*, 140.

- (11) Matsuoka, K.; Yamagishi, Y.; Yamazaki, T.; Setoyama, N.; Tomita, A.; Kyotani, T. *Carbon* **2005**, *43*, 876.

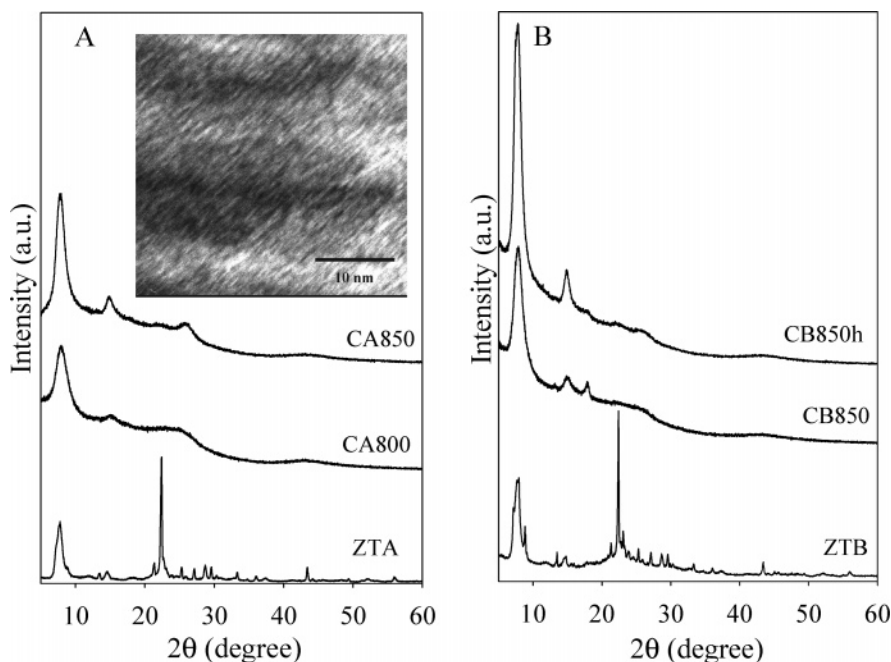


**Figure 1.** Powder XRD patterns of zeolite  $\beta$  templates and corresponding carbon materials prepared at various CVD temperatures. The intensity scale is the same for all samples. The inset in (A) shows a representative TEM image of sample CA850.

was observed.<sup>2b,8,12</sup> This is a significant finding because it has previously been accepted that close replication of zeolite  $\beta$  ordering in templated carbons is not possible due to the disordered structure of BEA-type zeolites.<sup>3,4</sup>

To confirm the reproducibility and efficacy of the nanocasting/replication process in generating zeolite-type structural ordering in templated carbons, we prepared carbon samples from a different zeolite  $\beta$  template. The XRD pattern of sample CB850 (Figure 1B) exhibits a high intensity “basal peak” at  $2\theta = 7^\circ$ , and a second peak at  $2\theta = 15^\circ$ , which is consistent with a high level of zeolite-type structural ordering. A third peak at  $2\theta = 18^\circ$  is observed for sample CB850, which is at a position similar to the (105) diffraction of the zeolite  $\beta$  template. We speculatively attribute this peak to zeolite-structural ordering, although we do not rule out the possibility that it may arise from other carbon contaminants (e.g.,  $C_{60}$ ). The higher intensities of the basal and second “zeolite” XRD peaks of sample CB850h (Figure 1B) indicate that zeolite-type structural ordering was enhanced by thermally treating the CVD derived zeolite/carbon composite in a nitrogen atmosphere.

The XRD patterns (Figure 1A) exhibit a broad and low-intensity peak at  $2\theta = 26^\circ$ , which is the (002) diffraction from turbostratic carbon. This indicates that the carbon materials are essentially amorphous and implies that most of the carbon precursor was deposited within the zeolite pores rather than on the external surface of the zeolite particles. The assumption here is that only carbon deposited on the external surface can undergo graphitization (formation of graphene sheets) due to the absence of any spatial limitations on the zeolite surface.<sup>2a</sup> On the other

hand, carbon deposited within the zeolite pores cannot undergo graphitization due to spatial limitations imposed by the size of the pores. In particular, the XRD patterns in Figure 1B show a remarkable lack of externally deposited (graphitic) carbon; no significant peak is observed at  $2\theta = 26^\circ$ .

The nitrogen sorption isotherms of the carbon materials and zeolite  $\beta$  template are shown in Figure 2. The pore size distribution (PSD) of some of the carbons is given in Figure 2B (inset). The nitrogen sorption isotherms of all of the carbon samples exhibit very high adsorption below  $P/P_0 = 0.1$ , which we ascribed to micropore filling. This suggests that a large proportion of the pore channels in the carbons are micropores, which is consistent with zeolite-like structural ordering. The isotherms also exhibit some nitrogen uptake at  $P/P_0 > 0.1$ , which may be attributed to adsorption into larger pores arising from interparticle voids. The isotherms exhibit hysteresis over a wide partial pressure range. Such hysteresis has previously been observed for some zeolite templated carbons.<sup>2</sup> The PSD curves (inset Figure 2B) exhibit a relatively sharp distribution of micropores dominated by pores in the range 0.5–0.9 nm with a maxima at ca. 0.6 nm. The pore size distribution is consistent with a significant level of microporosity in the carbons. Furthermore, pores of size between 0.5 and 0.9 nm, with a preponderance of pores of size ca. 0.6 nm, for the carbons is reasonable in light of the fact that the thickness of the zeolite wall framework (which becomes the pores in the carbons) is ca. 0.6 nm.<sup>2a</sup>

The textural properties of the carbon materials are summarized in Table 1. All samples have high surface area (2100–3200  $m^2/g$ ) and pore volume (1.7–2.5  $cm^3/g$ ). These textural properties are comparable to the highest ever reported for zeolite templated carbons.<sup>2b,4,12</sup> The carbons also exhibit high micropore surface area (1200–2400  $m^2/g$ ) and micropore volume (0.55–1.15  $cm^3/g$ ). We ascribe the high textural properties and microporosity to the zeolite-like structural ordering of the carbons. It is noteworthy that the microporosity of sample

(12) (a) Ma, Z.; Kyotani, T.; Tomita, A. *Carbon* **2002**, *40*, 2367. (b) Hou, P.-X.; Orikasa, H.; Yamazaki, T.; Matsuoka, K.; Tomita, A.; Setoyama, N.; Fukushima, Y.; Kyotani, T. *Chem. Mater.* **2005**, *17*, 5187. (c) Garsuch, A.; Klepel, O.; Sattler, R. R.; Berger, C.; Glaeser, R.; Wejtamp, J. *Carbon* **2006**, *44*, 593. (d) Garsuch, A.; Klepel, O. *Carbon* **2005**, *43*, 2330. (e) Ma, Z.; Kyotani, T.; Liu, Z.; Terasaki, O.; Tomita, A. *Chem. Mater.* **2001**, *13*, 4413. (f) Hou, P.-X.; Yamazaki, T.; Orikasa, H.; Kyotani, T. *Carbon* **2005**, *43*, 2624. (g) Ma, Z. X.; Kyotani, T.; Tomita, A. *Chem. Commun.* **2000**, 2365.



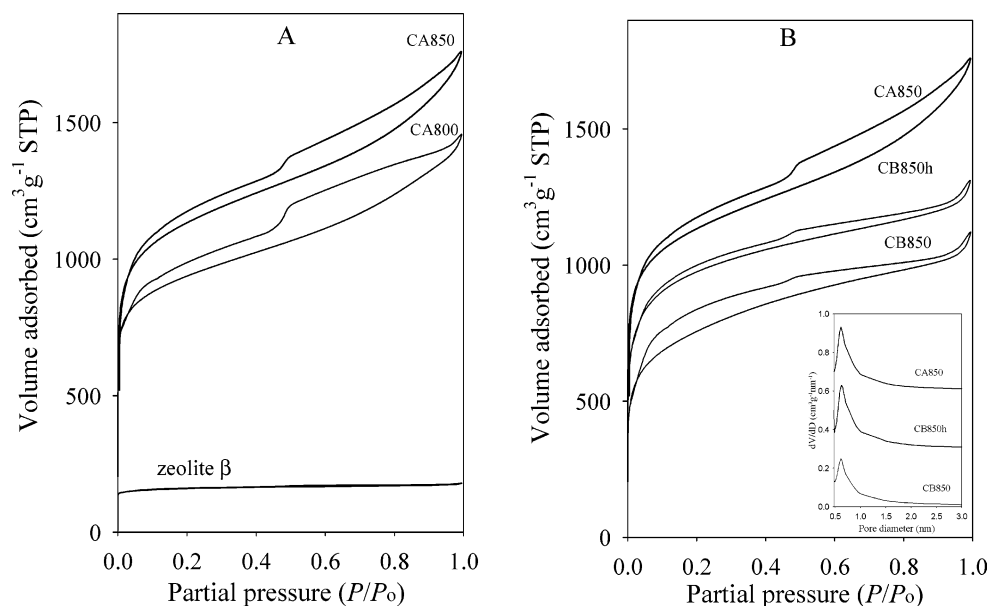


**Figure 2.** Nitrogen sorption isotherms of carbon materials prepared using zeolite  $\beta$  templates: (A) isotherms for samples prepared at 800 and 850 °C and (B) isotherms of samples prepared at 850 °C with and without additional heating. See Experimental Section for sample designation. The nitrogen sorption isotherm of one of the zeolite  $\beta$  templates (ZTA) is included for comparison. The inset in (B) shows the corresponding pore size distribution (PSD) curves calculated using the Horvath–Kawazoe (HK) model assuming slit pore geometry.

**Table 1.** Textural Properties and Hydrogen Uptake Capacity of Carbon Materials Prepared via CVD Using Zeolite  $\beta$  Templates

sample	surface area (m <sup>2</sup> /g) <sup>a</sup>	pore volume (cm <sup>3</sup> /g) <sup>b</sup>	H <sub>2</sub> uptake (wt %) <sup>c</sup>	max H <sub>2</sub> uptake (wt %) <sup>d</sup>
ZTA	527 (486)	0.28 (0.23)		
CA800	2191 (1213)	1.79 (0.56)	3.9	4.67
CA850	3189 (1529)	2.41 (0.71)	6.0	6.35
ZTB	342 (301)	0.23 (0.14)		
CB850	2611 (1150)	1.74 (0.79)	5.5	6.46
CB850h	3150 (2397)	1.95 (1.13)	6.9	8.33

<sup>a</sup> Values in parentheses are micropore surface area. <sup>b</sup> Values in parentheses are micropore volume. <sup>c</sup> Hydrogen uptake capacity at  $-196$  °C and 20 bar. <sup>d</sup> Maximum hydrogen uptake determined from Langmuir plots (Supporting Information Figure 4S).

CB850h, which had an extra heating step, is particularly high with a proportion of micropore surface area (76%) and pore volume (56%) that is higher than that of sample CB850 (45%), and closer to that of the zeolite templates (90% micropore surface area and 60–80% micropore volume). This suggests that the extra heating step enhances the formation of micropores.<sup>12a</sup>

Replication of zeolite-like structural ordering in the carbons requires extensive infiltration of the carbon precursor into the pores of the zeolite  $\beta$  template. The carbon yield is therefore important; in the absence of externally deposited carbon, we observed higher carbon yield at 850 than at 800 °C, which is consistent with the better ordering of sample CA850 as compared to that of CA800 (Figure 1A). Replication of zeolite structural ordering in the carbons was probed by microscopy. SEM images of the zeolite  $\beta$  template and sample CA850 (Figure 3) indicate that the morphology (shape and size) of the zeolite particles is replicated in the carbon material. Carbon particles with solid cores and smooth surfaces (Figure 3C) with hardly any irregular stand-alone particulates are formed. This differs from our previous observations where we obtained either hollow particles or solid core particles with rough surfaces and irregular particles (Supporting Information Figure 1S) for zeolite  $\beta$  templated carbons that had lower levels of zeolite-type

structural ordering, lower surface area, and in some cases high proportions of graphitic carbon.<sup>8</sup> An important variation in the preparation procedure is that in the previous report<sup>8</sup> the carbon precursor was in contact with the zeolite  $\beta$  template during both the temperature ramping process and the final heating step at the target CVD temperature. The CVD procedure used here, whereby the carbon precursor is in contact with the zeolite  $\beta$  template only after the final heating step is attained, appears to be better suited for replication of particle morphology from the zeolite to the carbons. The high level of zeolite-type structural ordering in the present carbon materials is confirmed by TEM analysis (inset in Figure 1A and Supporting Information Figure 2S). Ordered pore channels are observed with an estimated pore size of ca. 0.8 nm. The pore size estimated from the TEM images agrees with the pore size (0.5–0.9 nm) determined from nitrogen sorption data (inset in Figure 2B). The overall picture that emerges from the powder diffraction, porosity, and microscopy data is that a high level of zeolite-like structural ordering is replicated in the carbon materials.

**3.2. Hydrogen Uptake of the Zeolite-like Carbons.** The hydrogen uptake of the carbon materials was measured via two methods, gravimetric and volumetric. The hydrogen uptake, measured by gravimetric method with an IGA at  $-196$  °C over the pressure range 0–20 bar, is shown in Figure 4. We note that kinetic data on hydrogen adsorption indicated a rapid (2.5–3 min) achievement of equilibrium, which is consistent with a lack of any significant effects due to the presence of impurities. The carbon density (1.5 cm<sup>3</sup>/g) used in the buoyancy corrections was determined from helium sorption data obtained using the IGA at a pressure of up to 20 bar at 323 K. The hydrogen uptake isotherms were therefore calculated on the basis of a density of 1.5 g/cm<sup>3</sup> for the carbon samples, and hydrogen density of 0.04 g/cm<sup>3</sup> was used for buoyancy correction of adsorbed hydrogen.<sup>13</sup> (Supporting Information Figure 3S shows the hydrogen uptake

(13) (a) Kowalczyk, P.; Holyst, R.; Terzyk, A. P.; Gauden, P. A. *Langmuir* **2006**, *22*, 1970. (b) Wang, Q.; Johnson, J. K. *J. Chem. Phys.* **1999**, *110*, 577.

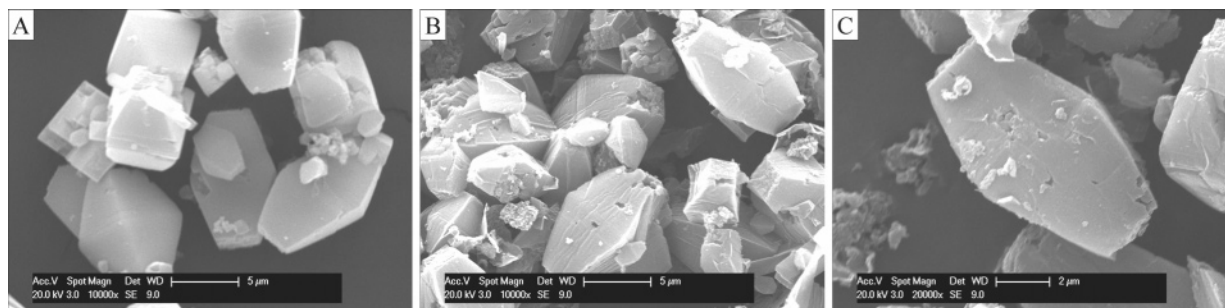


**Figure 3.** Representative SEM images of (A) zeolite  $\beta$  template (ZTA) and (B,C) ZTA-templated carbon (sample CA850) prepared at a CVD temperature of 850 °C.

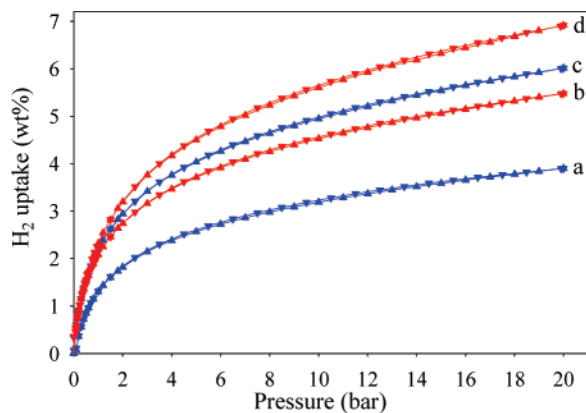


**Figure 4.** Hydrogen sorption isotherms at  $-196$  °C of carbons obtained via CVD using zeolite  $\beta$  as template and acetonitrile as carbon precursor: (a) CA800, (b) CB850, (c) CA850, (d) CB850h. (Carbon density of  $1.5$  g/cm<sup>3</sup> and hydrogen density of  $0.04$  g/cm<sup>3</sup> were used for buoyancy correction of adsorbed H<sub>2</sub>.)

isotherms in the absence of buoyancy correction for adsorbed hydrogen.) The isotherms do not exhibit any hysteresis, which confirms that the uptake of hydrogen by the carbon materials is reversible. Table 1 gives the hydrogen uptake capacity at a pressure of 20 bar. The uptake capacity at 20 bar varies between 4 and 7 wt %. (In the absence of buoyancy correction, the uptake at 20 bar is between 3.3 and 6 wt %.) However, it is clear that the isotherms indicate that saturation is not attained at 20 bar, and therefore higher uptake capacities are possible at pressure above 20 bar. Langmuir plots (Supporting Information Figure 4S) were used to predict the maximum uptake capacity, and the data are given in Table 1. The estimated maximum hydrogen uptake capacity varies between 4.67 wt % for CA800 and 8.33 wt % for CB850h. The hydrogen uptake capacity of up to 6.9 wt % (with an estimated maximum uptake of 8.33 wt %) observed for the present carbon materials is among the highest ever reported for carbon or any other porous material. Hirscher

and Panella recently examined hydrogen storage for a wide range of high surface area carbon nanostructures and reported a maximum capacity of 4.5 wt % at 70 bar.<sup>6a</sup> We have recently observed uptake of up to 4.5 wt % at 20 bar for zeolite-templated carbons with low levels of zeolite-type structural ordering.<sup>9</sup> The storage capacity of the present zeolite-like carbons is generally higher than that of metal organic frameworks (MOFs),<sup>14</sup> mesoporous carbons,<sup>6c,d</sup> zeolites,<sup>15</sup> or organic microporous polymers.<sup>16</sup>

To verify our hydrogen uptake measurements, we compared our data with that of well-known porous materials that have previously been investigated by other groups: a commercially available activated carbon (G212) and a metal organic framework (MOF-505). We found that the activated carbon G212 (surface area and pore volume of 1405 m<sup>2</sup>/g and 0.7 cm<sup>3</sup>/g, respectively) had an uptake of 2.0 wt % at 1 bar and 3.96 wt % at 20 bar (Supporting Information Figure 5S). This uptake very closely matches that obtained by Zhao et al.,<sup>6b</sup> who observed an uptake of 2.15 wt % at 1 bar for activated carbon G212. Under our hydrogen uptake measurement conditions, MOF-505 has been shown to have a hydrogen uptake of 2.6 wt % at 1 bar and 4.1 wt % at 20 bar.<sup>14i</sup> This uptake very closely agrees with the data by Yaghi and co-workers,<sup>14c</sup> who have recently reported hydrogen uptake of 2.47 wt % at 1 bar for MOF-505.

To further confirm the gravimetrically (IGA) determined hydrogen storage data, we performed volumetric (Micromeritics ASAP 2020) determination of hydrogen uptake capacity for sample CA850. The hydrogen uptake isotherms obtained via both methods agree closely as shown in Figure 5A, which attests to the veracity and reliability of our hydrogen uptake measurements. At 1 bar, the hydrogen uptake capacity for sample CA850 is determined to be 2.3 and 2.6 wt % via the gravimetric (IGA) and volumetric (ASAP 2020) methods, respectively. Moreover, we further confirmed the reliability of our hydrogen uptake measurements by performing uptake of deuterium via the gravimetric (IGA) method and comparing the uptake with that of hydrogen; the expected ratio of wt % uptake is 2:1 (D<sub>2</sub>:H<sub>2</sub>). This is indeed what we observed as shown in Figure 5B. Perhaps more importantly, we observed values of 1.08–1.16 for the molar ratio of adsorbed D<sub>2</sub>:H<sub>2</sub> (Supporting Information Figure

(14) (a) Panella, B.; Hirscher, M. *Adv. Mater.* **2005**, *17*, 538. (b) Rowsell, J. L. C.; Yaghi, O. M. *Angew. Chem., Int. Ed.* **2005**, *44*, 4670. (c) Chen, B.; Ockwig, N. W.; Millward, A. R.; Contreras, D. S.; Yaghi, O. M. *Angew. Chem., Int. Ed.* **2005**, *44*, 4745. (d) Rosi, N. L.; Eckert, J.; Eddaoudi, M.; Vodak, D. T.; Kim, J.; O'Keeffe, M.; Yaghi, O. M. *Science* **2003**, *300*, 1127. (e) Rowsell, J. L. C.; Millward, A. R.; Park, K. S.; Yaghi, O. M. *J. Am. Chem. Soc.* **2004**, *126*, 5666. (f) Zhao, X.; Xiao, B.; Fletcher, A. J.; Thomas, K. M.; Bradshaw, D.; Rosseinsky, M. *Science* **2004**, *306*, 1012. (g) Panella, B.; Hirscher, M.; Putter, H.; Muller, U. *Adv. Funct. Mater.* **2006**, *16*, 520. (h) Lee, J. Y.; Pan, L.; Kelly, S. P.; Jagiello, J.; Emge, T. J.; Li, J. *Adv. Mater.* **2005**, *17*, 2703. (i) Chun, H.; Dybtsev, D. N.; Kim, H.; Kim, K. *Chem.-Eur. J.* **2005**, *11*, 3521. (j) Wong-Foy, A. G.; Matzger, A. J.; Yaghi, O. M. *J. Am. Chem. Soc.* **2006**, *128*, 3494. (k) Frost, H.; Duren, T.; Snurr, R. A. *J. Phys. Chem. B* **2006**, *110*, 9565. (l) Lin, X.; Jia, J.; Zhao, X. B.; Thomas, K. M.; Blake, A. J.; Walker, G. S.; Champness, N. R.; Hubberstey, P.; Schroder, M. *Angew. Chem., Int. Ed.* **2006**, *45*, 7358.

(15) (a) Zecchina, A.; Bordiga, S.; Vitillo, J. G.; Ricchiardi, G.; Lamberti, C.; Spoto, G.; Bjorgen, M.; Lillerud, K. P. *J. Am. Chem. Soc.* **2005**, *127*, 6361. (b) Nijkamp, M. G.; Raaymakers, J. E. M. J.; van Dillen, A. J.; de Jong, K. P. *Appl. Phys. A* **2001**, *72*, 619. (16) McKeown, N. B.; Ghanem, B.; Msayib, K. J.; Budd, P. M.; Tattershall, C. E.; Mahmood, K.; Tan, S.; Book, D.; Langmi, H. W.; Walton, A. *Angew. Chem., Int. Ed.* **2006**, *45*, 1804.

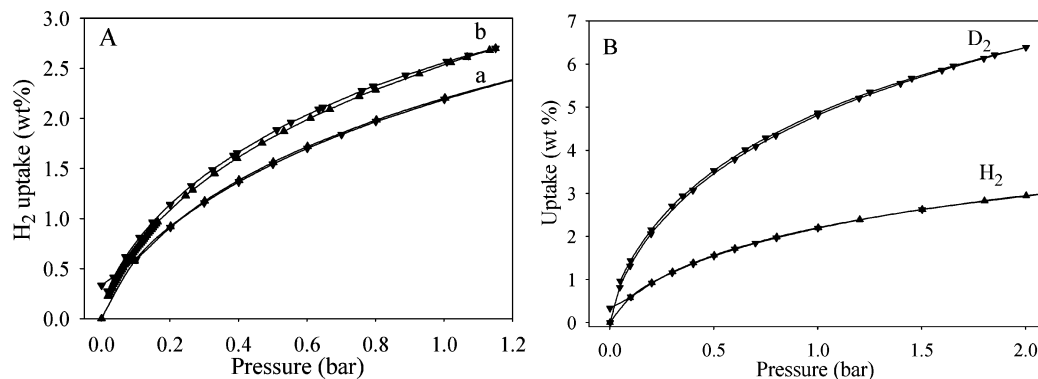


**Figure 5.** (A) Hydrogen sorption isotherms at  $-196\text{ }^{\circ}\text{C}$  of sample CA850 measured by (a) gravimetric and (b) volumetric methods. (B) Hydrogen and deuterium sorption isotherms of sample CA850. Sample density of  $1.5\text{ g/cm}^3$  was used, and hydrogen density of  $0.04\text{ g/cm}^3$  and deuterium density of  $0.08\text{ g/cm}^3$  were used for buoyancy correction of adsorbed  $\text{H}_2$  and  $\text{D}_2$ , respectively.

6S). This molar ratio is similar to that (1.06–1.10) observed for other types of porous carbons under comparable conditions.<sup>17</sup>

Samples prepared at  $850\text{ }^{\circ}\text{C}$ , which possess higher textural properties, have higher hydrogen uptake capacity. The hydrogen uptake capacity is therefore largely dependent on the textural properties of the carbon materials. High surface area and associated pore volume are clearly responsible for the enhanced hydrogen sorption. It is, however, noteworthy that the carbon (sample CB850h) with the highest hydrogen uptake has the highest micropore surface area and pore volume and the highest proportion of micropore surface area (76%) and pore volume (56%). This suggests that microporosity plays a beneficial role in hydrogen uptake and that the enhanced hydrogen sorption capacity of the present carbon samples is related to their zeolite-like structural ordering. Recent studies have shown that it is not just the overall surface area that influences hydrogen uptake in porous carbons, but the surface area associated with “optimal pores” of a specific size of ca.  $0.7\text{ nm}$ .<sup>6g,h,18</sup> In most activated carbons, the microporosity covers a wide range of pore size within the micropore range ( $0.3\text{--}2.0\text{ nm}$ ) in addition to the presence of mesopores.<sup>19</sup> Therefore, although the total surface area and microporosity of some activated carbons is high, the surface associated with “optimal pores” of size ca.  $0.7\text{ nm}$  is lower. For the present zeolite-like carbon materials, the microporosity is dominated by pores of size  $0.6\text{--}0.8\text{ nm}$  due to zeolite-type structural ordering. Thus, the surface area associated with “optimal pores” is also high, which translates to enhanced hydrogen uptake capacity.

Given that the adsorption of hydrogen on porous solids at  $-196\text{ }^{\circ}\text{C}$  is limited by its low interaction energy with the solid surfaces, it is likely that the preponderance of “optimal pores” of ca.  $0.7\text{ nm}$  size in the zeolite-like carbons improves the interaction by overlap of the potential fields from both sides of the pore. Pores wider than the optimal size will experience a decrease in the interaction energy with a concomitant decrease in hydrogen uptake. To explore the interaction between hydro-

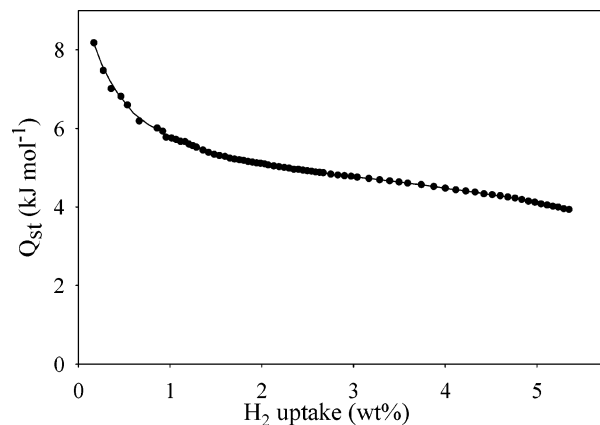


**Figure 6.** Isosteric heat of  $\text{H}_2$  adsorption ( $Q_{\text{st}}$ ) for carbon sample CB850h as a function of the amount of hydrogen adsorbed.

gen and the surface of the carbons, we calculated the isosteric heat of adsorption ( $Q_{\text{st}}$ ) using hydrogen sorption isotherms measured at two temperatures ( $-196$  and  $-186\text{ }^{\circ}\text{C}$ ). Calculation of the isosteric heat of adsorption was based on the Clausius–Clapeyron equation (Supporting Information Figure 7S). A plot of the isosteric heat of adsorption ( $Q_{\text{st}}$ ) as a function of hydrogen uptake is shown in Figure 6.  $Q_{\text{st}}$  varies from  $8.2\text{ kJ/mol}$  at low hydrogen uptake to  $4\text{ kJ/mol}$  at high uptake (i.e., higher surface coverage), and therefore as expected the heat of adsorption decreases at higher hydrogen uptake.<sup>18,20</sup> It is noteworthy that the initial isosteric heat of adsorption is as high as  $8.2\text{ kJ/mol}$ . This suggests a strong interaction between adsorbed hydrogen and the carbon surface. The initial isosteric heat of adsorption for the present carbon materials ( $8.2\text{ kJ/mol}$ ) is higher than that of activated carbon and metal organic framework materials.<sup>18,20</sup> It is likely that the presence of optimally sized pores and a relatively high heat of adsorption are responsible for the enhanced hydrogen uptake capacity of the zeolite-like carbons.

#### 4. Conclusions

In summary, we have prepared zeolite-like carbon materials that exhibit very high surface area via a CVD route using zeolite  $\beta$  as solid template. The zeolite-like structural ordering of the carbon materials is indicated by powder XRD patterns with at least two well-resolved diffraction peaks and TEM images showing well-ordered pore channels. Our findings show that it is possible to prepare carbon materials that have well-resolved zeolite-like XRD patterns using zeolites with disordered struc-

- (17) (a) Tanaka, H.; Kanoh, H.; Yudasaka, M.; Iijima, S.; Kaneko, K. *J. Am. Chem. Soc.* **2005**, *127*, 7511. (b) Zhao, X. B.; Villar-Rodil, S.; Fletcher, A. J.; Thomas, K. M. *J. Phys. Chem. B* **2006**, *110*, 9947.  
 (18) Yushin, G.; Dash, R.; Jagiello, J.; Fischer, J. E.; Gogotsi, Y. *Adv. Funct. Mater.* **2006**, *16*, 2288.  
 (19) (a) Ustinov, E. A.; Do, D. D.; Fenelonov, V. B. *Carbon* **2006**, *44*, 653. (b) Gauden, P. A.; Terzyk, A. P.; Rychlicki, G.; Kowalczyk, P.; Cwiertnia, M. S.; Garbacz, J. K. *J. Colloid Interface Sci.* **2004**, *273*, 39.  
 (20) (a) Benard, P.; Chahine, R. *Langmuir* **2001**, *17*, 1950. (b) Lee, J. Y.; Li, J.; Jagiello, J. *J. Solid State Chem.* **2005**, *178*, 2527. (c) Lee, J. Y.; Pan, L.; Kelly, S. P.; Jagiello, J.; Emge, T. J.; Li, J. *Adv. Mater.* **2005**, *17*, 2703.

ture such as zeolite  $\beta$  as template. The carbon materials exhibit enhanced (and reversible) hydrogen storage capacity, with measured uptake of up to 6.9 wt % and estimated maximum of 8.33 wt %. At lower pressure (1 bar), hydrogen uptake capacity of 2.6 wt % is achieved. Isothermic heat of adsorption of up to 8.2 kJ/mol indicates a strong interaction between adsorbed hydrogen and carbon surface. The hydrogen uptake capacity observed for the zeolite-like carbon materials is among the highest ever reported for carbon (activated carbon, mesoporous carbon CNTs) or any other (MOFs, zeolites) porous material.

**Acknowledgment.** We are grateful to the EPSRC for financial support.

**Supporting Information Available:** Seven additional figures: SEM and TEM images, hydrogen sorption isotherms with no buoyancy correction for adsorbed H<sub>2</sub>, Langmuir plots for H<sub>2</sub> adsorption, hydrogen sorption isotherms including a comparison with activated carbon, a plot showing the variation of the ratio of amounts adsorbed (molar  $nD_2/nH_2$  ratio) with pressure for zeolite-like carbon, and hydrogen sorption isotherms (obtained at  $-196$  and  $-186$  °C) used for calculating isothermic heat of adsorption. This material is available free of charge via the Internet at <http://pubs.acs.org>.

JA067149G